check for updates

ARTICLE

Early-Age Properties Development of Recycled Glass Powder Blended Cement Paste: Strengths, Shrinkage, Nanoscale Characteristics, and Environmental Analysis

Zhihai He[1,2], Menglu Shen[1], Jinyan Shi[3,*], Jingyu Chang[1], Víctor Revilla-Cuesta[4] and Osman Gencel[5]

[1]College of Civil Engineering, Shaoxing University, Shaoxing, 312000, China

[2]Key Laboratory of Rock Mechanics and Geohazards of Zhejiang Province, Shaoxing, 312000, China

[3]School of Civil Engineering, Central South University, Changsha, 410075, China

[4]Department of Civil Engineering, Escuela Politécnica Superior, University of Burgos, c/Villadiego s/n, Burgos, 09001, Spain

[5]Civil Engineering Department, Bartin University, Bartin, 74100, Turkey

[*]Corresponding Author: Jinyan Shi. Email: jinyan.shi@csu.edu.cn

ABSTRACT

Recycling solid waste in cement-based materials cannot only ease its load on the natural environment but also reduce the carbon emissions of building materials. This study aims to investigate the effect of recycled glass powder (RGP) on the early-age mechanical properties and autogenous shrinkage of cement pastes, where cement is replaced by 10%, 20% and 30% of RGP. In addition, the microstructure and nano-mechanical properties of cement paste with different RGP content and water to binder (W/B) ratio were also evaluated using SEM, MIP and nanoindentation techniques. The results indicate that the early-age autogenous shrinkage decreases with the increase of RGP content and W/B ratio. While the mechanical strength deteriorates due to the addition of RGP, it can be compensated by reducing the W/B ratio. Although the addition of RGP increases the total porosity of the hardened paste, it reduces the small size porosity (<50 nm). In addition, the proportions of different types of C-S-H are changed, and the volume fraction of porosity is increased, but that of hydration products of cement paste is reduced due to the incorporation of RGP. Besides its pozzolanic activity, the mitigated shrinkage deformation that RGP is generating in cement pastes is encouraging for its use as a novel supplementary cementitious material that reduces the early-age cracking risk of cement-based materials. Meanwhile, the life cycle assessments indicate that the RGP-cement component is an economical and eco-friendly novel engineering material.

KEYWORDS

Cement paste; waste glass powder; autogenous shrinkage; microstructure; nanoindentation

1 Introduction

Nowadays, Portland cement has become the most widely used binder for building materials [1–4]. However, cement production contributes to nearly 5%–7% of total anthropogenic CO_2 emissions [5]. Meanwhile, this effect is increasing, and the CO_2 emissions from cement production are projected to increase to 16%–24% by 2050 [5]. Therefore, there is an urgent need to enhance the sustainability of the

cement industry, so supplementary cementitious materials (SCMs) with hydraulic, filler or pozzolanic properties are used to partially replace cement. In the past, granulated blast-furnace slag (GBFS), limestone powder, fly ash (FA), etc., were used to replace cement, but due to their availability and production limitations, natural pozzolanic materials have been difficult to meet the growing demand for binders now [6–10]. Therefore, new SCMs need to be developed to replace cement.

The use of recycled glass powder (RGP) as a novel SCM has received considerable interest in recent years [11,12]. The RGP is obtained by grinding waste glass, which is used as a desirable SCM due to the high silica content and potential reactivity [11]. Some studies have shown that the pozzolanic effect of RGP can improve the properties of cement-based materials, especially durability [11]. Du et al. [13] revealed the mechanical properties and durability of concrete containing fine RGP in high volumes up to 60% as cement substitute, the results indicated that all concrete containing RGP exhibited higher strength than plain concrete due to the denser microstructure, and the permeability of harmful ion (Cl$^-$) and water was hindered in concrete with high volume RGP. Wang et al. found that the utilization of RGP reduced drying shrinkage of mortar with multiple fineness glass aggregates, and especially, 20% RGP as cement substitute inhibited successfully the deteriorative alkali-silica reaction (ASR) expansion induced by glass aggregates [10]. In addition, the research results of Sharifi et al. show that the incorporation of RGP reduced the drying shrinkage of concrete, while Kara et al. concluded the opposite result [14,15]. Kamali et al. [16] found that incorporation of RGP increased later mechanical properties of concrete and the impermeability of chloride, and effectively inhibited the expansion of ASR in the concrete, which was mainly due to the densification of microstructure from the pozzolanic properties of RGP. He et al. [17] revealed the effect of RGP on the creep of concrete, and found that the utilization of RGP obviously reduced the creep of concrete largely due to the increased proportion of high density calcium silicate hydrate (HD C-S-H). Based on the above analysis, the RGP also effectively improves some properties of concrete, and there is no potential risk of ASR expansion in RGP concrete, but there is very little research on autogenous shrinkage of cementitious materials containing RGP as a novel SCM [18,19].

Time-dependent deformations, such as drying and autogenous shrinkage, are one of the main factors affecting the long-term service performance of concrete material [17,20]. These deformations are ubiquitous in concrete, and can generate tensile stresses that cause severe cracking of the concrete. These deformation behaviors are closely related to the early performance evolution of concrete, including the formation of microstructures, volume stability, and strength development obtained through hydration reactions. Thermal deformation and autogenous deformation are common forms of early-age concrete deformation. The thermal deformation is mainly formed by the hydration heat release of the binder. Autogenous deformations are defined as volume changes occurring without any moisture loss to the external environment, and are generated by chemical shrinkage, self-desiccation, etc.

Autogenous shrinkage is an important component of shrinkages induced by the self-desiccation which does not contain any shrinkage because of loss of substances, and application of external force. Autogenous shrinkage of cement components is increased with the reduction of the water to binder (W/B) ratio. Autogenous shrinkage of concrete has predominated the overall shrinkage of UHPC with high content of binders and low W/B ratio [21]. The stress induced by high autogenous shrinkage results easily in the cracking of concrete material, especially at early ages, so as to reduce the strengths and durability of concrete. In addition, autogenous shrinkage is largely dependent on the W/B ratio, the component and content of binders, internal microstructure and curing conditions [21]. In order to reduce autogenous shrinkage, based on its mechanism, some techniques are proposed that mainly focus on the addition of SCMs, chemical admixtures, different types of fibers, as well as the optimization of mixture proportions [21]. The effect of SCMs on autogenous deformation is related to their mineral composition, and physical and chemical properties, which affect the mechanical properties, pore structure, chemical shrinkage and hydration rate of cementitious materials [22]. Most existing SCMs increase self-desiccation and

autogenous shrinkage by accelerating the hydration of the binder and refining the pore structure. In addition, as cement clinker is replaced, the dilution effect also reduces shrinkage. Therefore, the influence of different SCMs on the autogenous deformation of concrete depends on different factors. FA can effectively reduce the autogenous deformation of concrete due to its low C_3A content and reactivity [23]. Meanwhile, FA has a spherical structure, and retains less water than cement particles, so its free water content is higher [23]. In addition, highly reactive GBFS and silica fume increase the autogenous deformation of concrete. GBFS increases the chemical shrinkage of hardened cement paste, and its higher fineness also leads to the formation of finer pore structures [24]. In addition, the hardened cement paste with silica fume also has higher chemical shrinkage and smaller pore size, which leads to an increase in autogenous shrinkage. However, the research on the effect of RGP on the early-age deformation behavior of cement paste has not been reported in the literature.

Previous studies have discussed the basic properties of concrete mixed with RGP, but the performance of the cementitious component mixed with RGP, especially the autogenous shrinkage has not been comprehensively investigated. This study aims to understand the influence of different W/B ratios and RGP content on the early-age autogenous shrinkage, microstructure and nano-mechanical properties of cement paste. In order to explain the influence mechanism of RGP on the early-age strengths and autogenous shrinkage of cement paste, the scanning electron microscope (SEM), mercury intrusion porosimetry (MIP), and nanoindentation techniques were used to evaluate the development of the microstructure and nano-mechanical properties. The results help to promote the further application of RGP in concrete to some extent, especially at a low W/B ratio.

2 Experimental Details

2.1 Materials

Cement and RGP are used as binders in this study. The 42.5 ordinary Portland cement (OPC) was adopted, and its physical properties are presented in Table 1. The waste glass containers are washed, dried, crushed, ground and screened to obtain RGP. The chemical compositions of OPC and RGP are listed in Table 2. The main chemical composition of RGP is SiO_2, which is much more than that of OPC, but the content of Al_2O_3 and CaO of RGP is far less than that of OPC. Meanwhile, the SEM images of OPC and RGP are presented in Fig. 1, and the OPC and RGP have similar particle morphologies that show obvious irregular and angular shapes. A sample containing 20% RGP is used to characterize the strength activity index of RGP. The strength activity indexes of RGP at the ages of 7 and 28 days are 82.15% and 87.32%, respectively.

Table 1: Main physical property indexes of OPC

Water requirement of normal consistency (%)	Setting time (min)		Compressive strength (MPa)		Flexural strength (MPa)	
	Initial	Final	3 days	28 days	3 days	28 days
27.0	205	395	21.6	45.0	4.7	8.7

Table 2: Main chemical compositions of binders (wt. %)

Material	Al_2O_3	SiO_2	Fe_2O_3	TiO_2	CaO	MgO	SO_3	K_2O	LOI
OPC	8.70	35.72	4.71	0.41	32.53	2.08	2.14	1.18	11.76
RGP	0.24	92.64	0.05	0.03	4.53	2.37	0.02	0.03	—

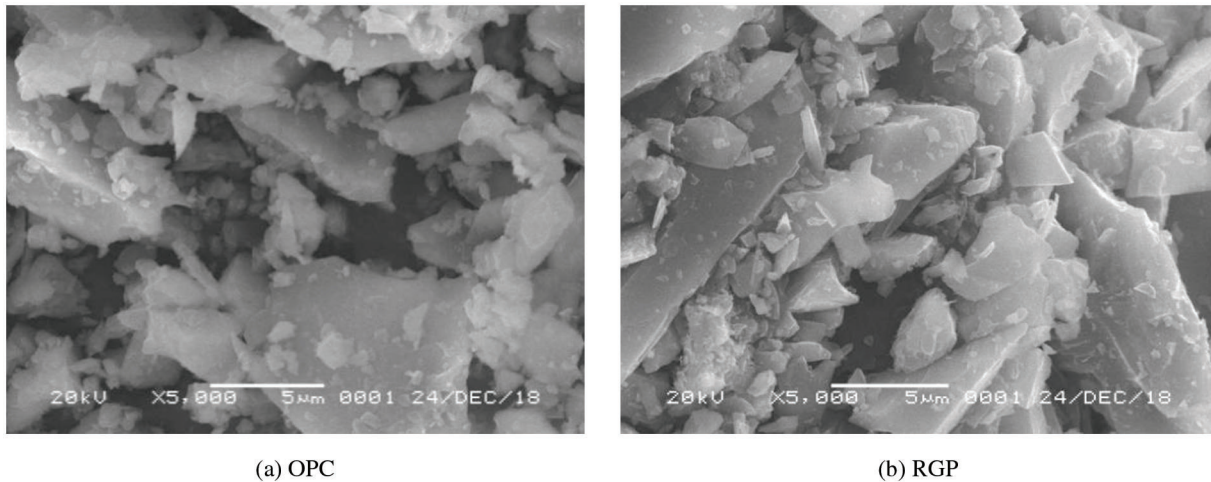(a) OPC   (b) RGP

Figure 1: SEM images of OPC and RGP

The median sizes of OPC and RGP are 24.4 μm and 19.8 μm, respectively, which shows that the average particle size of RGP is smaller than that of OPC, as presented in Fig. 2. When RGP is used as a cement substitute, it can also present micro aggregate effect. The polycarboxylate superplasticizer (SP) is used to adjust the fluidity of cement paste. The water-reducing ratio of SP is 25% and its solid content is about 40%.
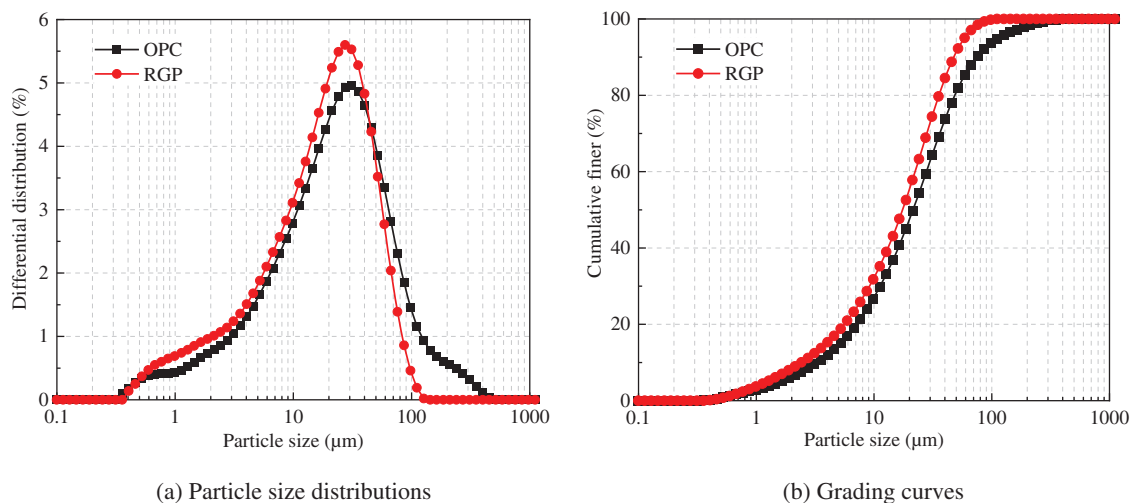

(a) Particle size distributions   (b) Grading curves

Figure 2: Particle size distribution of binders

2.2 Mixture Design and Preparation

Six types of cement pastes including, one reference group (B-0) and five groups with different W/B ratios and RGP content are designed and researched in this paper. The RGP is used to substitute OPC at incremental mass percentages of 10%, 20% and 30%, respectively. Meanwhile, the cement pastes containing 10% RGP with the different W/B ratios of 0.25–0.35 are also prepared to evaluate the autogenous shrinkage behavior of cement paste. Similar fluidity (240 ± 10 mm) of cement paste mixed with RGP is achieved by minor adjustment of SP. Table 3 gives mixed proportions of six pastes. For mixing, the OPC and RGP are poured into a mixer and mixed for 30 s, followed by the water with SP, which are stirred continuously for 2 min. After mixing, the fresh cement paste is cast into the mould

(40 mm × 40 mm × 160 mm). Next, the mould is placed in a standard curing room. The samples are demolded after one day and then continue to be cured until 3 and 7 days.

Table 3: Mix designs of the cement pastes

MIX ID	Binder proportion (%)		SP (wt. %)	W/B ratio
	OPC	RGP		
A-RGP-10	90	10	0.16	0.25
B-0	100	0	0.1	0.3
B-RGP-10	90	10	0.1	0.3
B-RGP-20	80	20	0.1	0.3
B-RGP-30	70	30	0.1	0.3
C-RGP-10	90	10	0.08	0.35

2.3 Test Methods

2.3.1 Mechanical Properties

The compressive and flexural strength tests are carried out using the specimens (40 mm × 40 mm × 160 mm) with and without RGP at 1, 3 and 7 days, respectively. The flexural and compressive tests are carried out in accordance with ASTM C348 and ASTM C349, respectively, and each strength value reported in the text is obtained from at least three specimens.

2.3.2 Autogenous Shrinkage

The corrugated tube method is used to investigate the autogenous shrinkage of the pastes according to ASTM C1698–2009. The YC-BWS autogenous shrinkage tester with a length of 430 mm and diameter of 29 mm is used in this study, as presented in Fig. 3. After mixing, the fresh paste is poured into the bellow. Three specimens are prepared and fixed on one shelf for each mixture. The start time of the test is the initial setting time of cement paste, and the setting time of the paste is determined according to BS EN 196-3:2005. Considering that most of the autogenous deformation is completed at an early age due to rapid development, the finish time of the test is 168 h, namely 7 days, after the initial setting time of cement paste.

Figure 3: Autogenous shrinkage tester

2.3.3 SEM and MIP

The microstructure of the specimen is observed through SEM (JSM-6360LV). The porosity of the specimen is measured through MIP. The samples of SEM and MIP tests are broken into small pieces at 7 days, and their sizes range from 3 to 5 mm. The selected pieces are immersed in isopropyl alcohol for 7 days to prevent further hydration, and then dried in a vacuum dryer for more than 7 days. The pore structure of samples is obtained by the Auto Pore IV 9510. Before SEM analysis, the gold-coating process is essential due to the poor electrical conductivity of inorganic material.

2.3.4 Nanoindentation Test

A cube piece with a side length of 20 mm is cut from the sample, and the steps of termination of hydration, epoxy impregnation, polishing and drying are performed in sequence, as shown in Fig. 4. During the polishing steps of different fineness (9, 3 and 0.25 μm), samples are cleaned using the ultrasonic instrument equipped with isopropyl alcohol. Surface polishing is repeated until the roughness of the sample is less than 300 μm.
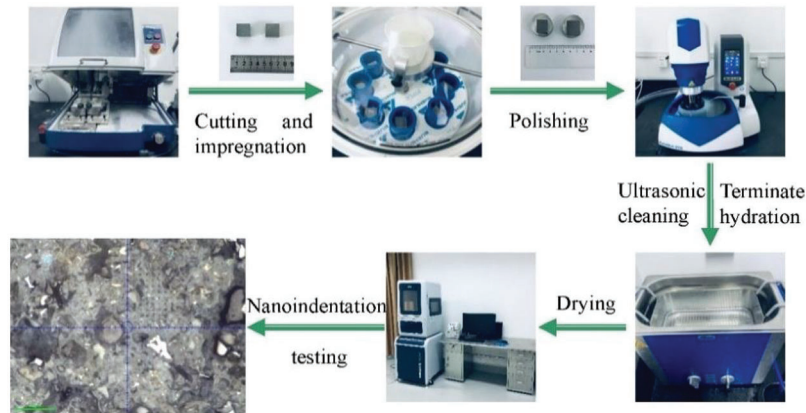

Figure 4: Process of nanoindentation test

For the nanoindentation test, Ti Premier (Bruker, Germany) equipped with a diamond tip is used in this study. During the test process, firstly, three representative areas in each specimen are chosen by the optical microscope of the nanoindentation apparatus, a 10×10 grid containing 100 points is designed in each area, and the distance is 10 μm. After that, a loading procedure is applied to the surface of the specimen, which includes initial loading at an increasing loading rate of 200 μN/s, followed by constant holding at the maximum load (2 mN) for 5 s, and then unloading at a constantly decreasing rate of 200 μN/s. After the test, the appearances of the tested specimen are shown in Fig. 5. Meanwhile, the elastic modulus of each indentation point which corresponds to one constituent phase can be calculated by the curves of indentation depth and load.
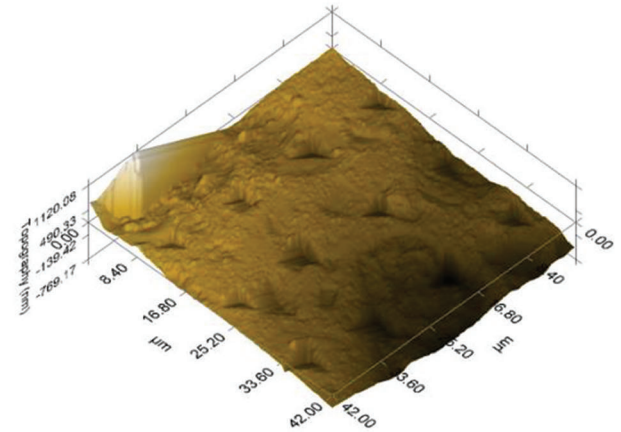
2.3.5 Life-Cycle Assessment

The life cycle assessment (LCA) fully considers the environmental effect of the product on the surrounding environment during creation, use, maintenance, and disposal [25]. The LCA of cement products containing RGP is calculated based on ISO 14040:2006 Environmental Management-Life Cycle Assessment-Principles and Framework and previous studies. Meanwhile, this study only considered the environmental impact of OPC and RGP in the collection, production, transportation and preparation process, and did not consider the environmental impact of cement products in the long-term service and maintenance process. The LCA is calculated through the SimaPro software, and some supplementary data

comes from the ecoinvent v3.1 database, which is finally calculated using the characterization factors specified in the U.S. Environmental Protection Agency (EPA) chemical and other environmental impact reduction and assessment tools (TRACI 2.1).
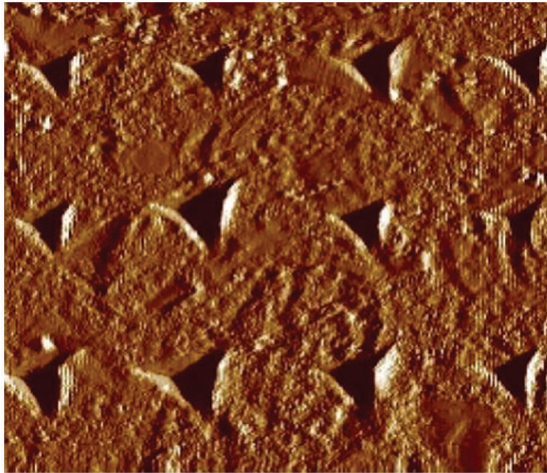
(a) Atomic force microscopy (AFM) image   (b) Surface topography

Figure 5: Appearance of tested area for nanoindentation test

3 Results and Discussions

3.1 Strength

3.1.1 Flexural Strength

Flexural strengths of hardened cement paste containing RGP with different W/B ratios at 1, 3 and 7 days are presented in Fig. 6. The incorporation of RGP significantly reduces the early-age flexural strength of hardened cement pastes, and the reduction level becomes more and more significant with the increase of RGP content. Compared with the control sample (B-0), the flexural strengths of cement paste containing 10% RGP at 1, 3 and 7 days are reduced by 13.3%, 17.7% and 10.5%, respectively. Flexural strengths of hardened cement paste containing 30% RGP are the lowest, only 5.4 MPa at 3 days and 8.5 MPa at 7 days, which should mainly be attributed to the decrease of hydration products caused by the decrease of cement content at early ages, especially before 7 days (Fig. 6b). In addition, W/B ratio has a significant influence on the flexural strength variations of hardened cement paste containing 10% RGP. The flexural strength gradually increases as the W/B ratio decreases, which is mainly due to the coarsening of the pore structure of the sample. Meanwhile, the flexural strength of hardened paste containing 10% RGP with the W/B ratio of 0.25 is close to that of control cement paste, which, in particular, surpasses that of the control sample at 1 day.

3.1.2 Compressive Strength

The compressive strengths of hardened cement paste containing RGP with different W/B ratios at 1, 3 and 7 days are obtained as presented in Fig. 7. The variation tendency of compressive strengths of samples containing RGP is similar to that of flexural strengths. The RGP reduces the early-age compressive strength of the sample, and with the increase of RGP content, the reduction is more and more obvious. With the reduction of the W/B ratio, the compressive strengths are increased. However, the compressive strengths of the sample containing 10% RGP with the W/B ratio of 0.25 at 1, 3 and 7 days surpass those of the control sample, respectively. Meanwhile, the strength reduction at early ages due to the incorporation of RGP can be compensated by reducing the W/B ratio. Similar results have been

reported. Wang et al. found that the utilization of 25% RGP to replace cement reduced the strengths at 7 and 28 days, especially at an early age [26]. Taha et al. confirmed that when RGP replaced 20% Portland cement, an average reduction of 16% in compressive strength of concrete was obtained [27].
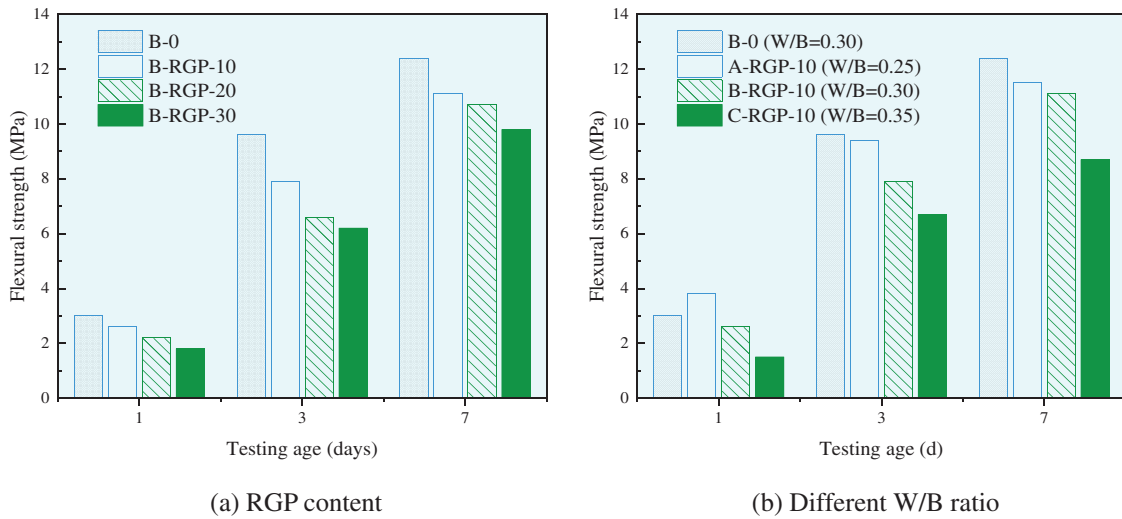

(a) RGP content   (b) Different W/B ratio

Figure 6: Influence of RGP on flexural strengths of samples with different W/B ratio

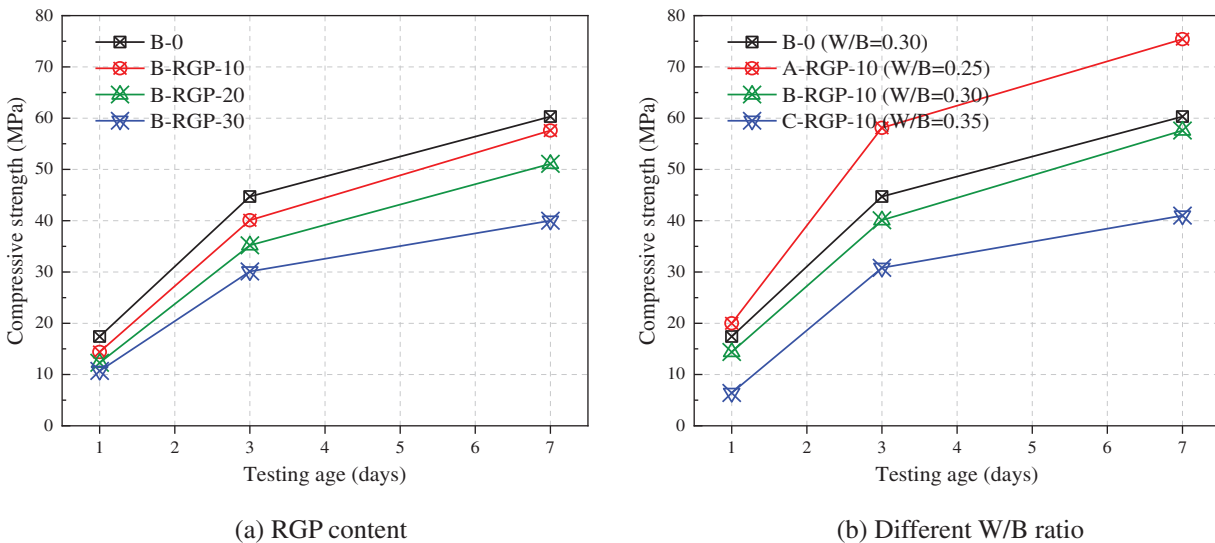(a) RGP content   (b) Different W/B ratio

Figure 7: Influence of RGP on compressive strengths of cement paste with different W/B ratio

3.2 Autogenous Shrinkage

During the autogenous shrinkage test, the data are automatically collected by the computer every 3 h in the first 3 days, and collected every 24 h after 3 days. The autogenous shrinkage of cement paste containing RGP with different W/B ratios is presented in Fig. 8.
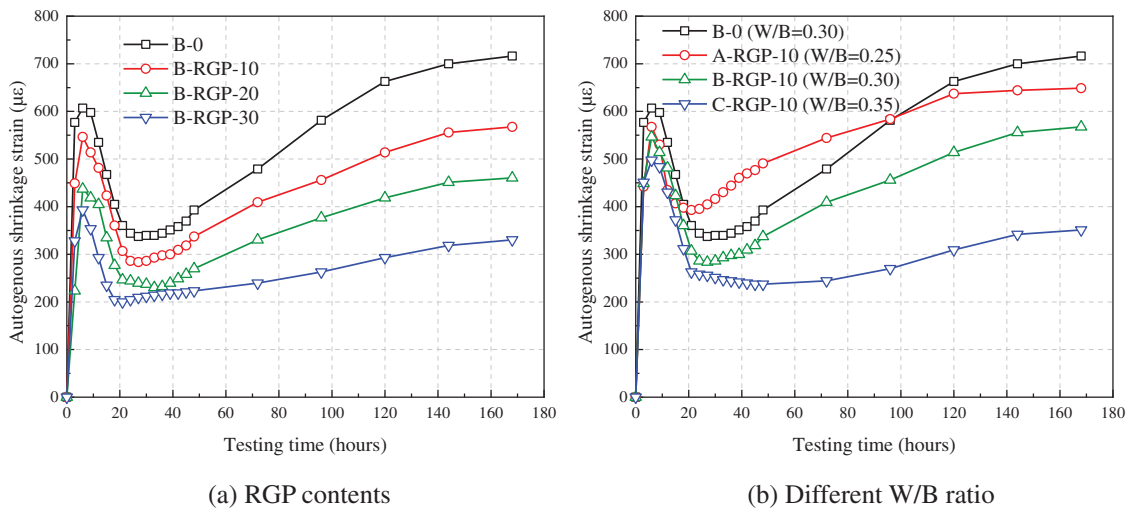
(a) RGP contents   (b) Different W/B ratio

Figure 8: Influence of RGP on autogenous shrinkage of cement paste with different W/B ratio

Fig. 8 presents the autogenous shrinkage behaviors of cement paste containing RGP, and it can be divided into three stages. The first stage is the rapid development stage of autogenous shrinkage from the start time to the 9th hour. In this stage, the stiffness and strength of cement paste are too low to restrain the volume change. Meanwhile, the hydration reaction of the binder is very fast, which leads to an increase in self-desiccation and chemical shrinkage. However, it is also considered that the shrinkage in this stage is the plastic shrinkage due to the fluidity and plasticity of cement paste before its rigid skeleton [28]. The second stage is the expansion stage of deformation from the 9th hour to the 24th hour. At this stage, the autogenous shrinkage of the paste is compensated to some extent. This may be due to the following effects; reabsorption of detrimental bleeding water accumulated at a very early age between paste and the corrugated tube; ettringite needles growth; crystals of calcium hydroxide growth; the topochemical reaction of C_3S [29]. When the expansion deformation is greater than autogenous shrinkage, the final deformation at this stage shows the expansion. In addition, while the autogenous shrinkage is tested for long ages more than 28 days, the expansion deformation at this stage is sometimes not obtained due to the low value and short duration time. The third stage is called the slow development stage of autogenous shrinkage after 24 h. With the increase of age, the hydration reaction becomes slow and the rigid skeleton is gradually formed, which can effectively restrain the volume deformation and lead to the slow development of autogenous shrinkage.

When RGP is used as a partial replacement of OPC, the autogenous shrinkage of cement paste is significantly reduced, as presented in Fig. 8a. Meanwhile, the decreasing trend becomes more and more obvious as the substitution ratio of RGP increases. Compared with the control cement paste without RGP (B-0) at 168 h (7 days), autogenous shrinkage of cement paste containing 10%, 20% and 30% RGP reduces by 20.8%, 35.8% and 53.9%, respectively. The reduction of autogenous shrinkage of paste is caused by many aspects. When OPC is replaced by RGP, the content of C_3A in the cement paste decreases. Second, the ratio of water to cement increases, which means that more water is used for cement hydration [29]. Therefore, the use of RGP to replace part of the cement reduces the autogenous shrinkage of the paste, and as the substitution ratio of RGP increases, the autogenous shrinkage of the paste decreases. In addition, according to Fig. 8b, the W/B ratio has a great effect on the autogenous shrinkage of cement paste, and with the reduction of the W/B ratio, the autogenous shrinkage of the sample containing 10% RGP is gradually increased. The three stages of autogenous shrinkage development of the control sample with a W/B ratio of 0.25 are different from that of the sample with

10% RGP. Compared with the control cement paste without RGP at 168 h (7 days), autogenous shrinkage of cement paste containing 10% RGP with the W/B ratio of 0.25, 0.3 and 0.35 reduced by 9.5%, 20.8% and 51.0%, respectively. This is mainly because of different microstructures caused by the W/B ratio.

3.3 Microstructure Analysis

3.3.1 Morphology and Mineralogy Analyses

The properties of cementitious materials containing strengths, shrinkage, creep and durability are largely dependent on the microstructure. The morphology and distribution of hydration products and different types of pores are important components of microstructure. Therefore, the SEM images of the sample with different RGP content at 7 days are presented in Fig. 9.
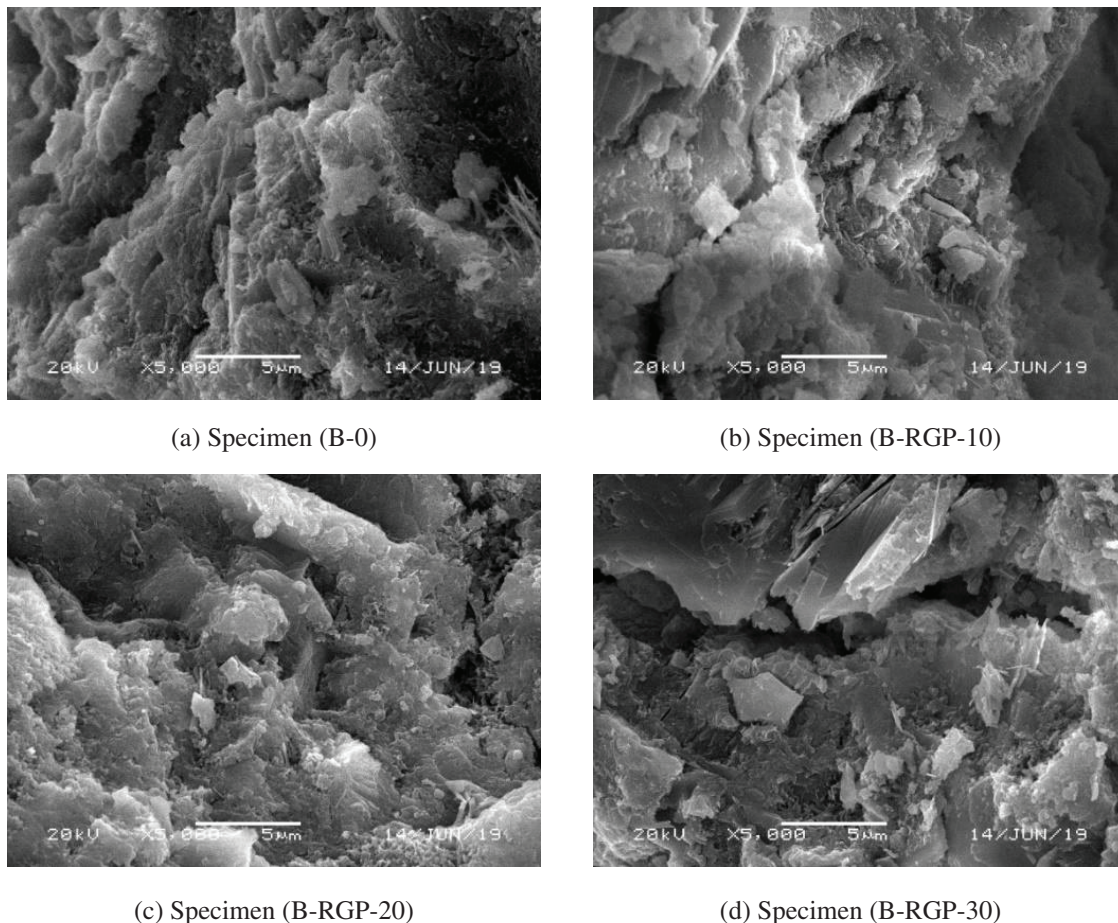

(a) Specimen (B-0)   (b) Specimen (B-RGP-10)

(c) Specimen (B-RGP-20)   (d) Specimen (B-RGP-30)

Figure 9: SEM images of cement paste

The microstructure of hardened cement paste at 7 days mainly consists of various hydration products, micro-cracks, pores, and some unhydrated particles (Cement clinker and RGP), as presented in Fig. 9. The incorporation of RGP has a significant effect on the microstructure compactness of cement paste. The sufficient hydration products, such as C-S-H and $Ca(OH)_2$, are easily found in the control cement paste, which overlaps each other to form the denser microstructure without obvious macropores and microcracks. It indicates that the hydration reaction of cement is relatively fast and mature, which well complies with the highest strength and autogenous shrinkage. When RGP is used as a partial replacement

of cement, some disconnected capillary pores are discovered in the microstructure of the sample containing 10% RGP due to the fewer hydration products. In addition, some angular unhydrated particles are also observed, but it is difficult to distinguish between cement and RGP because of their similar shapes. It, to some extent, corresponds with the delayed hydration reaction, and reduced strengths and autogenous shrinkage. With the increase of RGP content, the loose microstructure is further aggravated in cement paste containing 20% RGP. Some unhydrated particles and scattered hydration products are still found, the sizes of air voids and capillary pores gradually increase, and the lengths of microcracks become longer and their widths broaden. The incorporation of 30% RGP results in the large air voids and capillary pores, especially microcracks interconnecting to form some channels because of the lack of adequate hydration products, by which the microstructure is basically divided into several scattered pieces. It agrees with the lowest strengths and autogenous shrinkage due to the lowest hydration reaction of cementitious materials.

Fig. 10 presents SEM images of specimens with 10% RGP at different curing ages. The microstructure of the sample with 10% RGP is looser and has fewer hydration products. Meanwhile, RGP particles with a smooth surface can be found, and there are fewer hydration products in the sample at 1 day (Fig. 10a). As the curing age increases, the microstructure of the specimen becomes denser, and AFt is found in the sample at 3 days. In 7 days, products such as C-S-H gel and $Ca(OH)_2$ overlap with unhydrated particles to form a relatively dense microstructure, as shown in Fig. 10c.
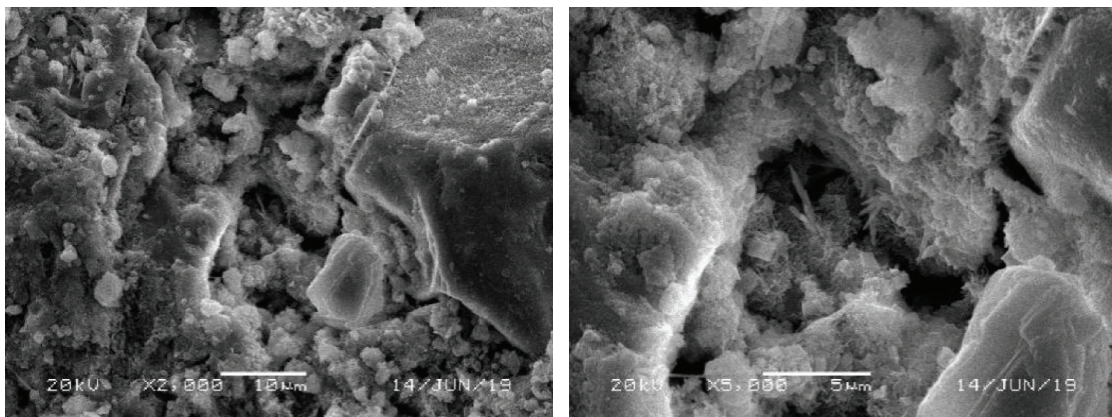
(a) 1 days
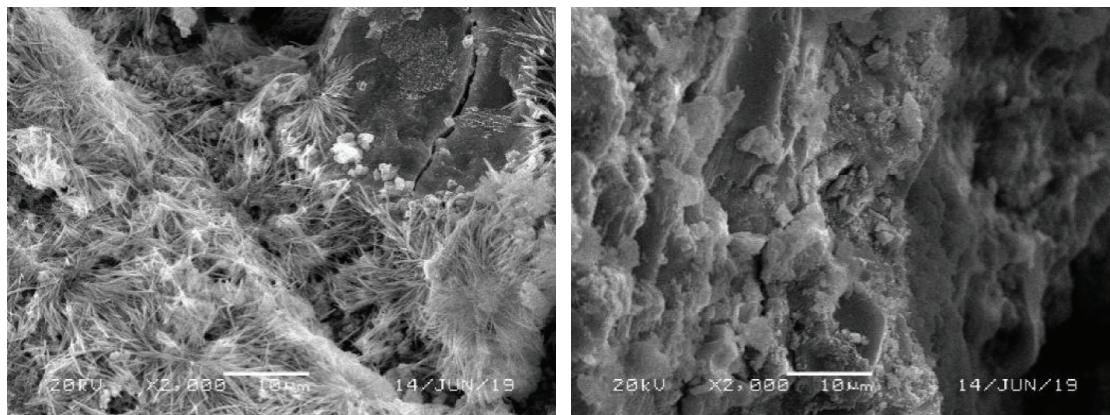
(b) 3 days   (c) 7 days

Figure 10: SEM images of B-RGP-10 sample at 1, 3 and 7 days

3.3.2 Pore Structure

The pore structure mainly containing the porosity and pore size distribution is also one of the determined influential factors in the shrinkage deformation of cementitious materials [21]. Ghafari et al. [30] reported that the content of fine pores in UHPC highly affected autogenous deformation, which was significantly reduced by reducing the fine pores in UHPC containing FA or GBFS, and there were also strong relationships between the autogenous deformation and porosity. Therefore, the influence of RGP content on the pore structure of the sample at 7 days is investigated by the MIP technique, and the results are presented in Fig. 11. Meanwhile, based on the above results, the effect of RGP contents on the pore size distribution can also be calculated, as shown in Table 4.
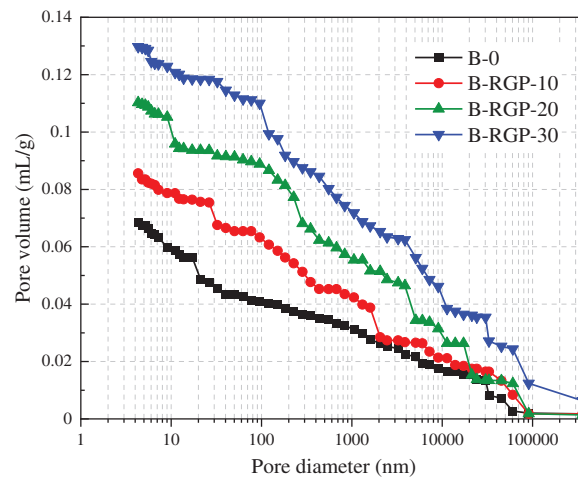

Figure 11: The influence of RGP content on porosity of cement paste

Table 4: Influence of RGP on pore size distributions of cement paste

Number	<50 nm	(50–100) nm	>100 nm	Total porosity
B-0	0.0252	0.0024	0.0408	0.0685
B-RGP-10	0.0202	0.0022	0.0633	0.0856
B-RGP-20	0.0189	0.0025	0.0889	0.1103
B-RGP-30	0.0169	0.0028	0.1100	0.1297

When RGP is used as a partial replacement of cement, the total porosity of the cement pastes is significantly increased as shown in Fig. 11 and Table 4. Meanwhile, the increase in porosity becomes more and more obvious as the RGP content increases, which complies with the SEM image results in Fig. 9. According to the different sizes, the total porosity of cement paste containing RGP can be divided into three types as follows: the porosity with the diameter smaller than 50 nm; the porosity with the diameter from 50 to 100 nm; the porosity with the diameter greater than 100 nm. The proportion of the porosity with a diameter greater than 100 nm in the total porosity is the greatest. However, there are only fine pores that can effectively affect autogenous shrinkage. The smaller the diameters are, the more obvious the effect is [30]. With the increase of RGP content, the porosity with a diameter greater than 100 nm as harmful pores increases gradually, which corresponds with the reduced strengths in Figs. 6 and 7. The incorporation of RGP in cement paste has no obvious effect on the porosity with the diameter

from 50 to 100 nm, which is clearly related to the filling effect and the potential pozzolanic reactivity of RGP. However, with the increase of RGP content, the porosity with a diameter smaller than 50 nm reduces gradually, which is consistent with the reduced autogenous shrinkage of cement paste in Fig. 8.

3.4 Nano-Mechanical Properties

Generally speaking, the content and evolution of C-S-H have a direct and important effect on the volume deformation of cementitious materials [31]. According to the different nanomechanical properties, C-S-H can be divided into three types as follows: ultra-high density C-S-H (UHD C-S-H), HD C-S-H and low density C-S-H (LD C-S-H) [20]. Therefore, the nanoindentation technique is employed to quantitatively obtain the variation of constituent phases. Each constituent phase has a relatively stable range of nanomechanical properties, and as for cementitious materials, the elastic moduli of CH, HD C-S-H, and LD C-S-H are in the range of 35–50, 24–35 and 14–24 GPa, respectively [17]. However, because CH and UHD C-S-H have similar nanomechanical properties, it is difficult to distinguish them by elastic modulus. Meanwhile, the constituent phase with an elastic modulus less than 14 GPa is regarded as the pore. In addition, the constituent phase with an elastic modulus of more than 50 GPa is considered as the unhydrated particles, such as the glass with an elastic modulus of 86.17 GPa [31]. The curves of indentation depth and a load of the typical constituent phase are shown in Fig. 12.
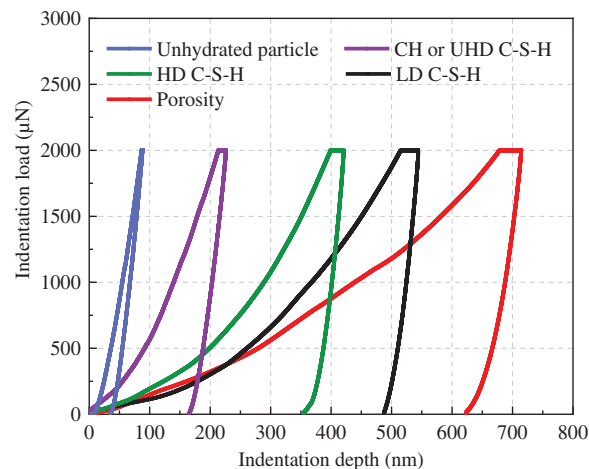

Figure 12: Typical curves of indentation depth and the load of constituent phases

After a few irregular curves of indentation depth and load are discarded, the contour maps of elastic modulus of the sample with RGP at 7 days are obtained by the rest of the curves, as shown in Fig. 13. The contour maps of elastic modulus of cement paste are totally different, which indicates the great effect of RGP.

Meanwhile, the effective elastic modulus values are collected to obtain the frequency histograms of the elastic modulus of the sample with RGP, as shown in Fig. 14.

According to the intrinsic nanomechanical properties of each constituent phase and the results of Fig. 14, the volume fraction variations of the main constituent phases of cement paste containing RGP are shown in Table 5. The incorporation of RGP has a great effect on the volume fraction variations of constituent phases, and the maximal volume fraction of the constituent phase of the control sample is HD C-S-H, but the maximal volume fraction of the sample containing RGP is LD C-S-H, as presented in Fig. 14 and Table 5. Compared to the control sample at 7 days, the incorporation of RGP increases the content of porosity and LD C-S-H, and however, reduces the volume fractions of HD C-S-H, CH or UHD C-S-H

and unhydrated particles, and with the increase of RGP content, the effect is more obvious [32]. The increased content of porosity due to the utilization of RGP complies with the reduced strengths of cement paste shown in Figs. 6 and 7. In addition, CH can not be distinguished from UHD C-S-H only by the nanoindentation tested results because of the similar nanomechanical property ranges. The incorporation of RGP changes the proportions of different types of C-S-H, and reduces the content of hydration products of cement paste at 7 days due to the cement dilution of RGP, which are the sum of LD C-S-H, HD C-S-H and CH or UHD C-S-H. This illustrates the delay in the hydration reaction, which is consistent with the autogenous shrinkage variations in Fig. 8. Finally, the volume fraction variations of unhydrated particles of cement paste seem unusual. The control cement paste should have the lowest volume fraction of unhydrated particles due to the fast hydration reaction of cement, and however, in fact, its value is the highest. This should be mainly attributed to the specific gravity of cement is greater than that of RGP, and when RGP is used to replace cement by weight, the volume of cement paste containing RGP increases. This may also be related to the dilution effect of RGP, which increases the hydration degree of the cement particles, thereby reducing the content of the unhydrated phase. However, during the nanoindentation test, the same areas and test points are adopted for all specimens which may lead to the above unusual results.
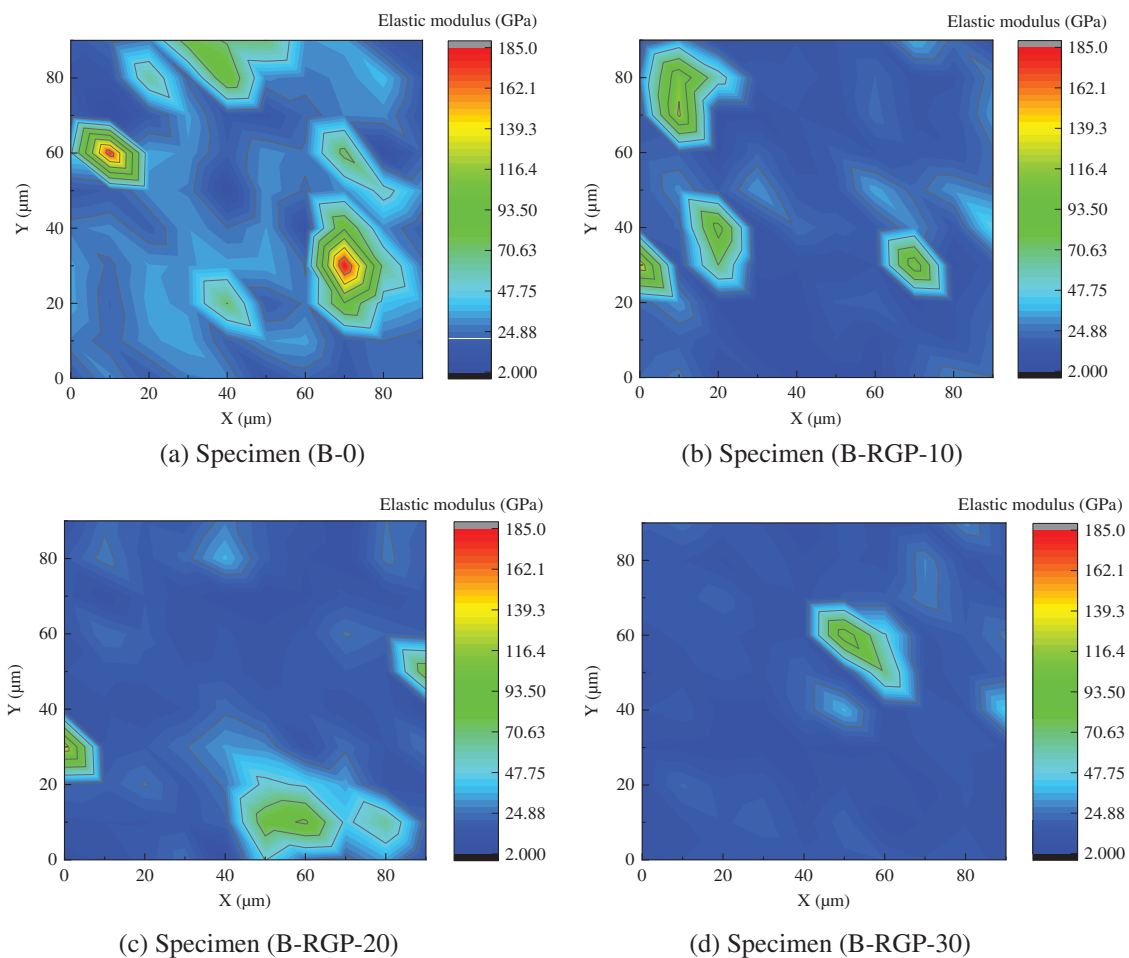

(a) Specimen (B-0)

(b) Specimen (B-RGP-10)

(c) Specimen (B-RGP-20)

(d) Specimen (B-RGP-30)

Figure 13: Effect of RGP on contour maps of elastic modulus of cement paste
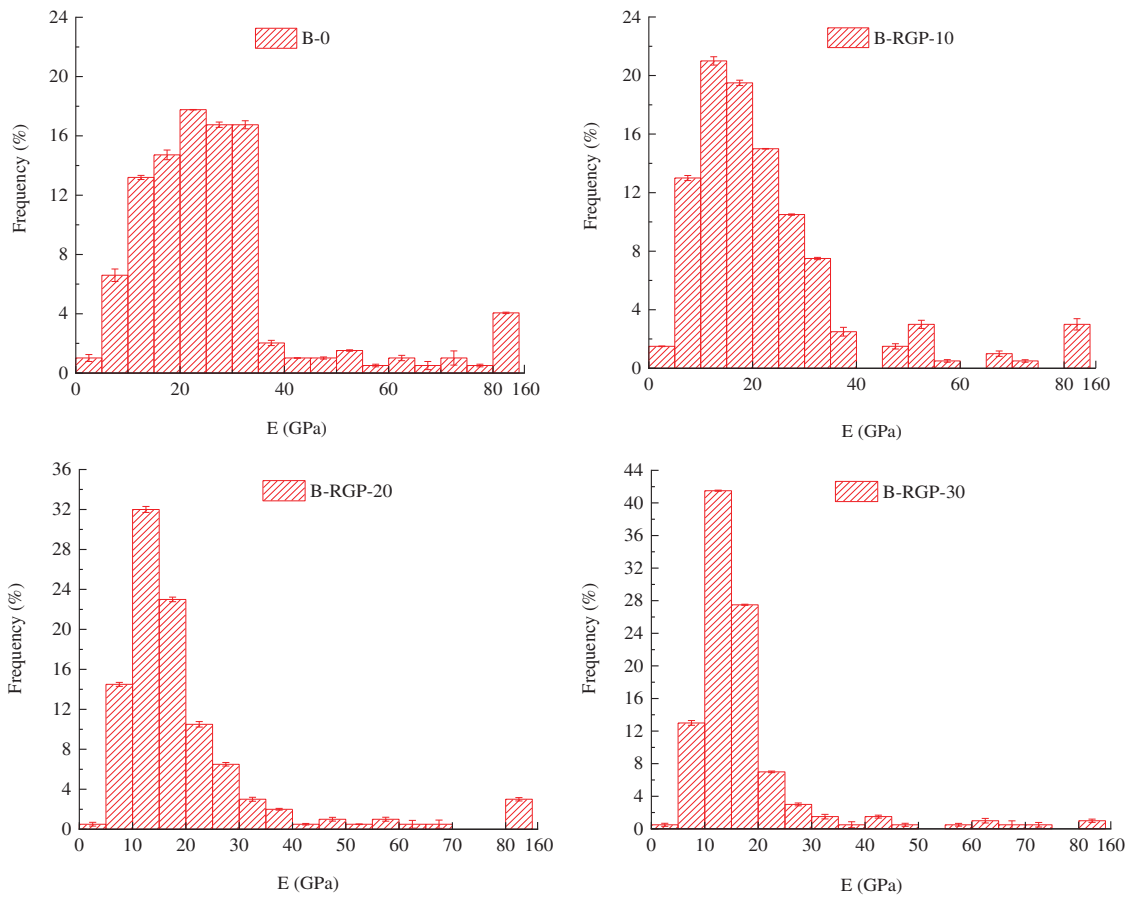
Figure 14: Effect of RGP on frequency histograms of elastic modulus of sample

Table 5: Effect of RGP on volume fractions of constituent phases of sample (%)

Specimen	Unhydrated particle	CH or UHD C-S-H	HD C-S-H	LD C-S-H	Porosity
B-0	10.5	4	37.5	31	17
B-RGP-10	8	3.5	21	34.5	33
B-RGP-20	6.5	3.5	11	42	37
B-RGP-30	3.5	2.5	6	44.5	43.5

3.5 Life-Cycle Assessment

The LCA results of the cement paste containing RGP are presented in Table 6. The incorporation of RGP can effectively reduce the environmental burden of cement-based materials on the surrounding environment. When part of OPC is replaced by RGP, the environmental impact of the mixture is lower than that of plain OPC paste. As expected, as the replacement ratio of RGP increases, the environmental load of the specimen becomes lower. When the substitution ratio of RGP is 30%, the formation potential of tropospheric ozone of the mixture is reduced by 27.35%, and global warming potential is reduced by 28.38%. Furthermore, the ozone depletion potential is reduced by 29.60%, the eutrophication potential is reduced by 28.70%, and the acidification potential is reduced by 22.93%. Although the incorporation of RGP reduces the early-age strength of cement paste, a proper amount of RGP can improve its long-term strength [17,33,34]. Meanwhile, the incorporation of RGP significantly reduces the early autogenous shrinkage of the cement

paste. When the cement product meets the requirements of the specification, using an appropriate amount of RGP instead of OPC can improve its environmental benefits. Of course, since RGP is a solid waste, its cost is also significantly lower than OPC. Therefore, the cement paste mixed with RGP also has good economic and social benefits, which is beneficial to the goals of sustainable development and carbon neutrality.

Table 6: The environmental impact of cement paste containing RGP

Per metric tonne of material	OPC (B-0)	RGP	RGP10	RGP20	RGP30
Formation potential of tropospheric ozone (kg O_3-eq.)	48.5	3.55	44.279	39.758	35.237
Global warming potential (100 years, kg CO_2-eq.)	1041	58.5	941.87	843.74	745.61
Ozone depletion potential (kg CFC 11-eq.)	0.000026	0.000000115	0.0000235016	0.0000209032	0.0000183048
Eutrophication potential (kg N-eq.)	1.21	0.027	1.1009	0.9818	0.8627
Acidification potential (kg SO_2-eq.)	2.42	0.5	2.255	2.06	1.865
Non-renewable primary energy: Fossil (MJ)	5250	1080	4833	4416	3999

4 Conclusions

In this work, the effect of RGP replacing cement by weight on the flexural and compressive strengths as well as autogenous shrinkage of cement paste with different W/B ratios was investigated. Meanwhile, MIP, SEM and nanoindentation techniques were carried out to support the findings and mechanism. The conclusions can be obtained as follows:

(1) The utilization of RGP reduces the strengths of cement paste at an early age, and the reduced strengths can be compensated by reducing the W/B ratio. When the W/B ratio is reduced from 0.30 to 0.25, the early-age compressive strength of the sample is significantly higher than that of the control sample.

(2) The autogenous shrinkage of cement paste experiences three stages within 7 days. The autogenous shrinkage of the pastes is decreased by the incorporation of RGP. Dilution and the formation of different hydration products are responsible for the low deformation ratio of the sample containing RGP.

(3) Based on SEM and pore structure results, the utilization of RGP degrades the microstructure of cement paste at early ages but reduces the porosity with a diameter smaller than 50 nm, which has the determined effect on the variation of autogenous shrinkage.

(4) Compared to the control sample at 7 days, the utilization of RGP changes the proportions of different types of C-S-H, and increases the volume fraction of porosity, but reduces that of hydration products of cement paste, which indicates the delayed hydration reaction.

(5) The results clearly show the potential of RGP as an alternative SCM for the production of cement-based materials. The incorporation of RGP reduces the early-age deformation of cement paste. This is beneficial to reduce the risk of early-ages cracking of the concrete, thereby improving the long-term service performance of concrete.

(6) The life cycle assessment also confirmed that using an appropriate amount of RGP to replace OPC to prepare cement products has better environmental benefits. When 10%–30% OPC is replaced by

RGP, the carbon emissions of cement paste are reduced by 9.5%–28.4% compared to plain UHPC (0% RGP).

Conflicts of Interest: The authors declare that they have no conflicts of interest to report regarding the present study.

References

1. Cheng, Z., Zhao, J., Cui, L. (2022). Exploration of hydration and durability properties of ferroaluminate cement with compare to portland cement. *Construction and Building Materials, 319,* 126138.

2. Liu, S., Shen, Y., Wang, Y., Shen, P., Xuan, D. et al. (2022). Upcycling sintering red mud waste for novel superfine composite mineral admixture and CO_2 sequestration. *Cement and Concrete Composites, 129,* 104497.

3. Ling, T. C., Poon, C. S., Wong, H. W. (2013). Management and recycling of waste glass in concrete products: Current situations in Hong Kong. *Resources, Conservation and Recycling, 70,* 25–31.

4. Wang, Y., Xiao, J., Zhang, J. (2022). Effect of waste marble powder on physical and mechanical properties of concrete. *Journal of Renewable Materials, 10(10),* 2623–2637. DOI 10.32604/jrm.2022.019381.

5. Wu, R., Zhao, T., Zhang, P., Yang, D., Liu, M. et al. (2021). Tensile behavior of strain hardening cementitious composites (SHCC) containing reactive recycled powder from various C&D waste. *Journal of Renewable Materials, 9(4),* 743–765. DOI 10.32604/jrm.2021.013669

6. He, P., Zhang, B., Yang, S., Ali, H. A., Lu, J. X. et al. (2020). Recycling of glass cullet and glass powder in alkali-activated cement: Mechanical properties and alkali–silica reaction. *Waste and Biomass Valorization, 11(12),* 7159–7169.

7. Wang, Y., Luo, S., Yang, L., Ding, Y. (2021). Microwave curing cement-fly ash blended paste. *Construction and Building Materials, 282,* 122685.

8. Shi, J., Liu, Y., Xu, H., Peng, Y., Yuan, Q. et al. (2022). The roles of cenosphere in ultra-lightweight foamed geopolymer concrete (UFGC). *Ceramics International, 48(9),* 12884–12896.

9. He, Z. H., Han, X. D., Shi, J. Y., Aslani, F., Gencel, O. et al. (2022). Multi-scale characteristics of eco-friendly marine binder using coral waste. *Powder Technology, 403,* 117395.

10. Wang, Y., He, H., Wang, J., Li, F., Ding, Y. et al. (2022). Effect of aggregate micro fines in machine-made sand on bleeding, autogenous shrinkage and plastic shrinkage cracking of concrete. *Materials and Structures, 55(3),* 1–15.

11. Letelier, V., Tarela, E., Osses, R., Cárdenas, J. P., Moriconi, G. (2017). Mechanical properties of concrete with recycled aggregates and waste glass. *Structural Concrete, 18(1),* 40–53. DOI 10.1002/suco.201500143.

12. Hou, S., Duan, Z., Ma, Z., Singh, A. (2020). Improvement on the properties of waste glass mortar with nanomaterials. *Construction and Building Materials, 254,* 118973. DOI 10.1016/j.conbuildmat.2020.118973.

13. Du, H., Tan, K. H. (2017). Properties of high volume glass powder concrete. *Cement and Concrete Composites, 75,* 22–29. DOI 10.1016/j.cemconcomp.2016.10.010.

14. Sharifi, Y., Afshoon, I., Firoozjaei, Z., Momeni, A. (2016). Utilization of waste glass micro-particles in producing self-consolidating concrete mixtures. *International Journal of Concrete Structures and Materials, 10(3),* 337–353. DOI 10.1007/s40069-016-0141-z.

15. Kara, P., Borosnyói, A., Fenyvesi, O. (2014). Performance of waste glass powder (WGP) supplementary cementitious material (SCM)–drying shrinkage and early age shrinkage cracking. *Epitoanyag Journal of Silicate Based and Composite Materials, 66,* 18–22. DOI 10.14382/epitoanyag-jsbcm.2014.4.

16. Kamali, M., Ghahremaninezhad, A. (2015). Effect of glass powders on the mechanical and durability properties of cementitious materials. *Construction and Building Materials, 98,* 407–416. DOI 10.1016/j.conbuildmat.2015.06.010.

17. He, Z. H., Zhan, P. M., Du, S. G., Liu, B. J., Yuan, W. B. (2019). Creep behavior of concrete containing glass powder. *Composites Part B: Engineering, 166,* 13–20. DOI 10.1016/j.compositesb.2018.11.133.

18. Patel, D., Shrivastava, R., Tiwari, R. P., Yadav, R. K. (2021). The role of glass powder in concrete with respect to its engineering performances using two closely different particle sizes. *Structural Concrete, 22,* E228–E244. DOI 10.1002/suco.201900182.

19. Zheng, K. (2016). Pozzolanic reaction of glass powder and its role in controlling alkali–silica reaction. *Cement and Concrete Composites, 67,* 30–38. DOI 10.1016/j.cemconcomp.2015.12.008.

20. He, Z. H., Shen, M. L., Shi, J. Y., Yalçınkaya, Ç., Du, S. G. et al. (2022). Recycling coral waste into eco-friendly UHPC: Mechanical strength, microstructure, and environmental benefits. *Science of the Total Environment, 836,* 155424. DOI 10.1016/j.scitotenv.2022.155424.

21. Yang, L., Shi, C., Wu, Z. (2019). Mitigation techniques for autogenous shrinkage of ultra-high-performance concrete–A review. *Composites Part B: Engineering, 178,* 107456. DOI 10.1016/j.compositesb.2019.107456.

22. Gedam, B. A., Bhandari, N. M., Upadhyay, A. (2016). Influence of supplementary cementitious materials on shrinkage, creep, and durability of high-performance concrete. *Journal of. Materials in Civil Engineering, 28(4),* 04015173. DOI 10.1061/(ASCE)MT.1943-5533.0001462.

23. Xie, T., Fang, C., Ali, M. M., Visintin, P. (2018). Characterizations of autogenous and drying shrinkage of ultra-high performance concrete (UHPC): An experimental study. *Cement and Concrete Composites, 91,* 156–173. DOI 10.1016/j.cemconcomp.2018.05.009.

24. Mounanga, P., Bouasker, M., Pertue, A., Perronnet, A., Khelidj, A. (2011). Early-age autogenous cracking of cementitious matrices: Physico-chemical analysis and micro/macro investigations. *Materials and Structures, 44(4),* 749–772. DOI 10.1617/s11527-010-9663-z.

25. Huntzinger, D. N., Eatmon, T. D. (2009). A life-cycle assessment of portland cement manufacturing: Comparing the traditional process with alternative technologies. *Journal of Cleaner Production, 17(7),* 668–675. DOI 10.1016/j.jclepro.2008.04.007.

26. Wang, Z., Shi, C., Song, J. (2009). Effect of glass powder on chloride ion transport and alkali-aggregate reaction expansion of lightweight aggregate concrete. *Journal of Wuhan University of Technology-Mater. Sci. Ed., 24(2),* 312–317. DOI 10.1007/s11595-009-2312-0.

27. Taha, B., Nounu, G. (2008). Properties of concrete contains mixed colour waste recycled glass as sand and cement replacement. *Construction and Building Materials, 22(5),* 713–720. DOI 10.1016/j.conbuildmat.2007.01.019.

28. Tao, J., Wei, X., Luo, Y. (2019). Comparison of non-contact autogenous shrinkage measurements and the stress ratio of capillary stress to compressive strength. *Construction and Building Materials, 206,* 226–235. DOI 10.1016/j.conbuildmat.2019.02.003.

29. de Sensale, G. R., Ribeiro, A. B., Gonçalves, A. (2008). Effects of RHA on autogenous shrinkage of portland cement pastes. *Cement and Concrete Composites, 30(10),* 892–897. DOI 10.1016/j.cemconcomp.2008.06.014.

30. Ghafari, E., Ghahari, S. A., Costa, H., Júlio, E., Portugal, A. et al. (2016). Effect of supplementary cementitious materials on autogenous shrinkage of ultra-high performance concrete. *Construction and Building Materials, 127,* 43–48. DOI 10.1016/j.conbuildmat.2016.09.123.

31. del Bosque, I. S., Zhu, W., Howind, T., Matías, A., de Rojas, M. S. et al. (2017). Properties of interfacial transition zones (ITZs) in concrete containing recycled mixed aggregate. *Cement and Concrete Composites, 81,* 25–34. DOI 10.1016/j.cemconcomp.2017.04.011.

32. Berodier, E. S. K. S. G., Scrivener, K. (2014). Understanding the filler effect on the nucleation and growth of C-S-H. *Journal of the American Ceramic Society, 97(12),* 3764–3773. DOI 10.1111/jace.13177.

33. Bian, Y., Li, Z., Zhao, J., Wang, Y. (2022). Synergistic enhancement effect of recycled fine powder (RFP) cement paste and carbonation on recycled aggregates performances and its mechanism. *Journal of Cleaner Production, 344,* 130848. DOI 10.1016/j.jclepro.2022.130848.

34. Zhao, J., Tong, L., Li, B., Chen, T., Wang, C. et al. (2021). Eco-friendly geopolymer materials: A review of performance improvement, potential application and sustainability assessment. *Journal of Cleaner Production, 307,* 127085. DOI 10.1016/j.jclepro.2021.127085.